Supplementary information for: Structure of an APC3-APC16 complex: Insights into assembly of the Anaphase Promoting Complex/Cyclosome

(a)

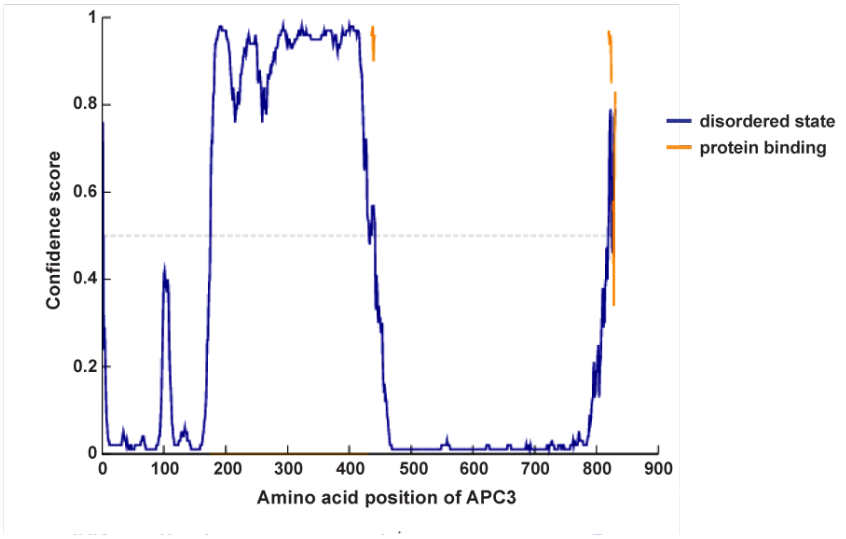

(b)

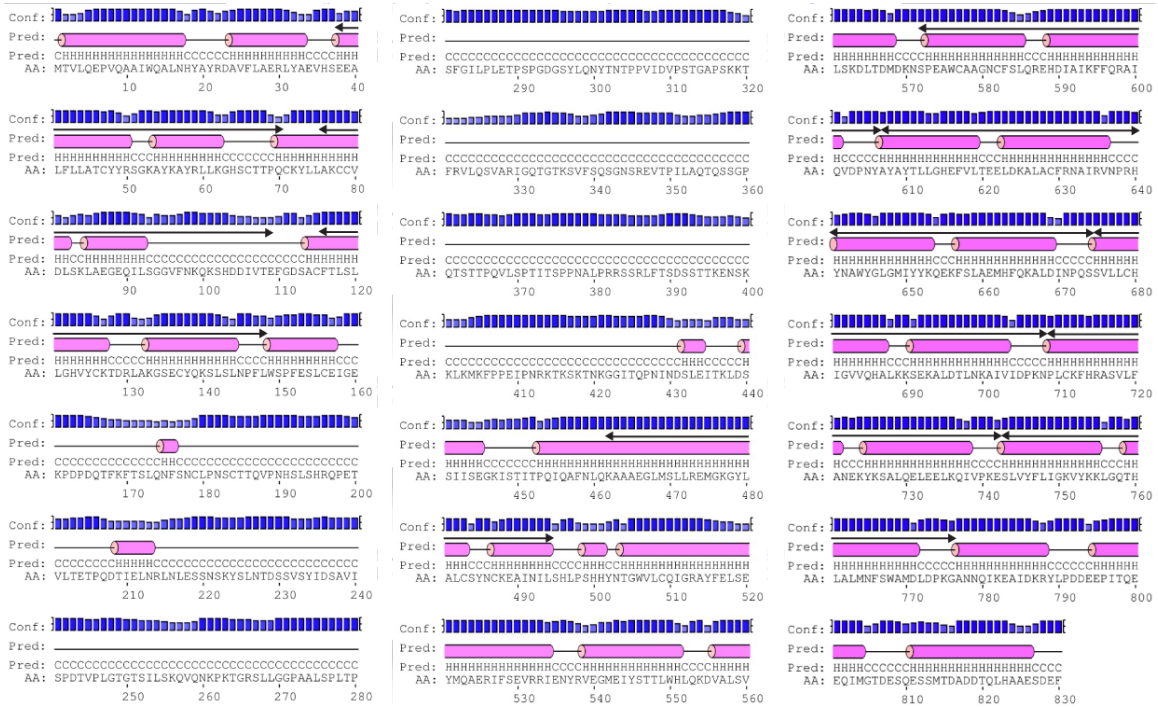

Figure S1. Secondary structure prediction for human APC3
(a) Disorder prediction for human APC3 using DISOPRED3[1]. Residues 175-471 and 819-830 are predicted to be disordered.

(b) Predicted secondary structure of human APC3 (PSI-PRED v3.3[1]) is shown with predicted TPRs (TPRpred[2]) as black double-headed arrows.

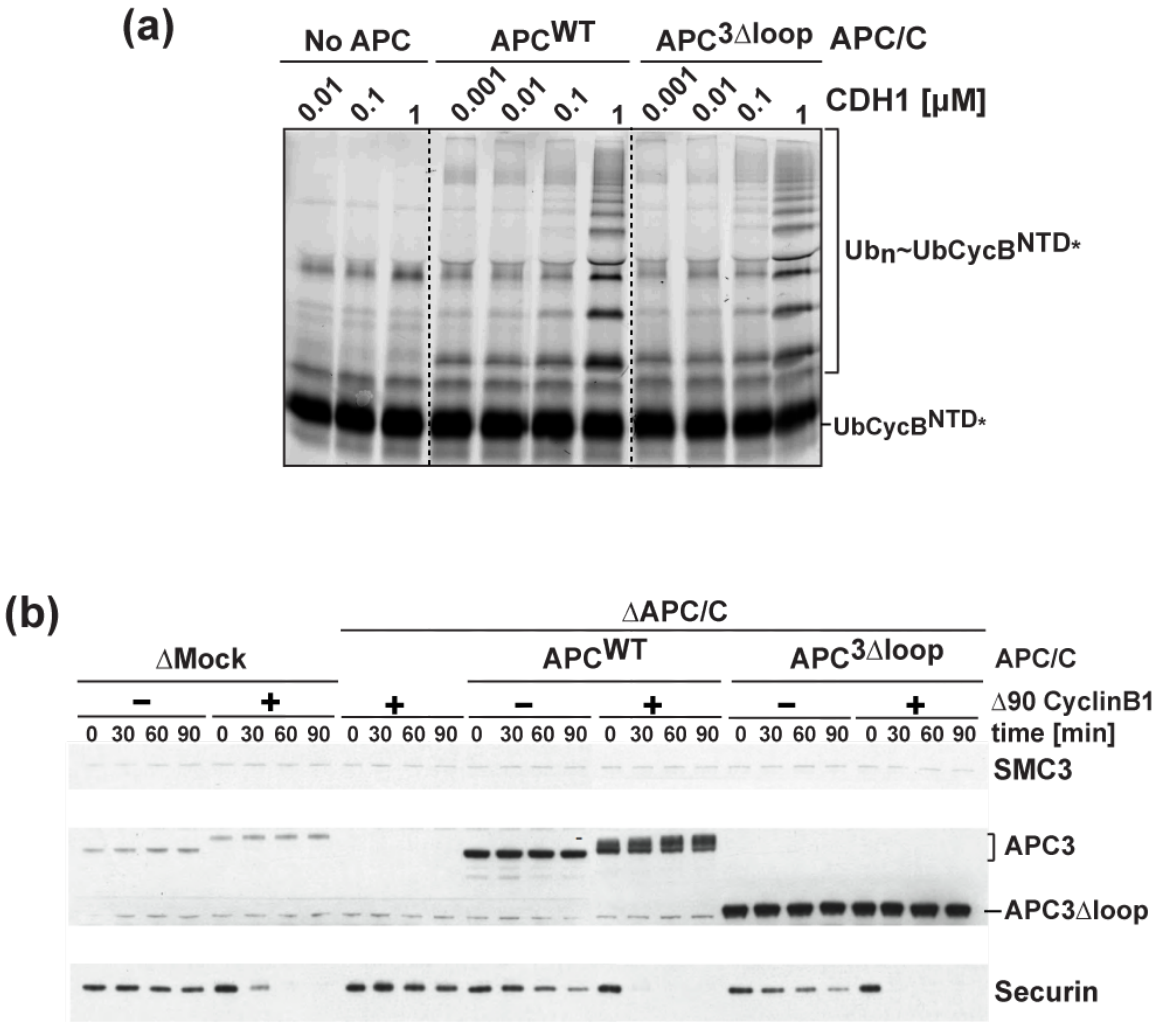

Figure S2. Activity of APC/C and APC/C with APC3Δloop
(a) Fluorescence scans of APC/C ubiquitination assays with increasing concentrations of CDH1. Assays use the E2 UBE2S and monitor ubiquitination of fluorescent Ub-CyclinB^{NTD*}.

(b) CDK-dependent substrate degradation in *X. laevis* egg extracts. The level of Securin substrate was monitored in extracts with or without adding nondegradable Δ90 CyclinB1 to activate CDK1. Wild-type APC3 is phosphorylated on several residues between 182-453, which are deleted in the mutant with APC3Δloop. Phosphorylated APC3 migrates more slowly on a gel. After depleting extracts of wild-type APC/C, Securin levels were monitored after adding back wild-type APC/C or the mutant with APC3Δloop. It is noted that according to the quantification of APC3 that there might be up to 30% more of the mutant as compared to wild-type APC/C, which could enable a wild-type rate of substrate degradation for experiments with APC/C harboring APC3Δloop.

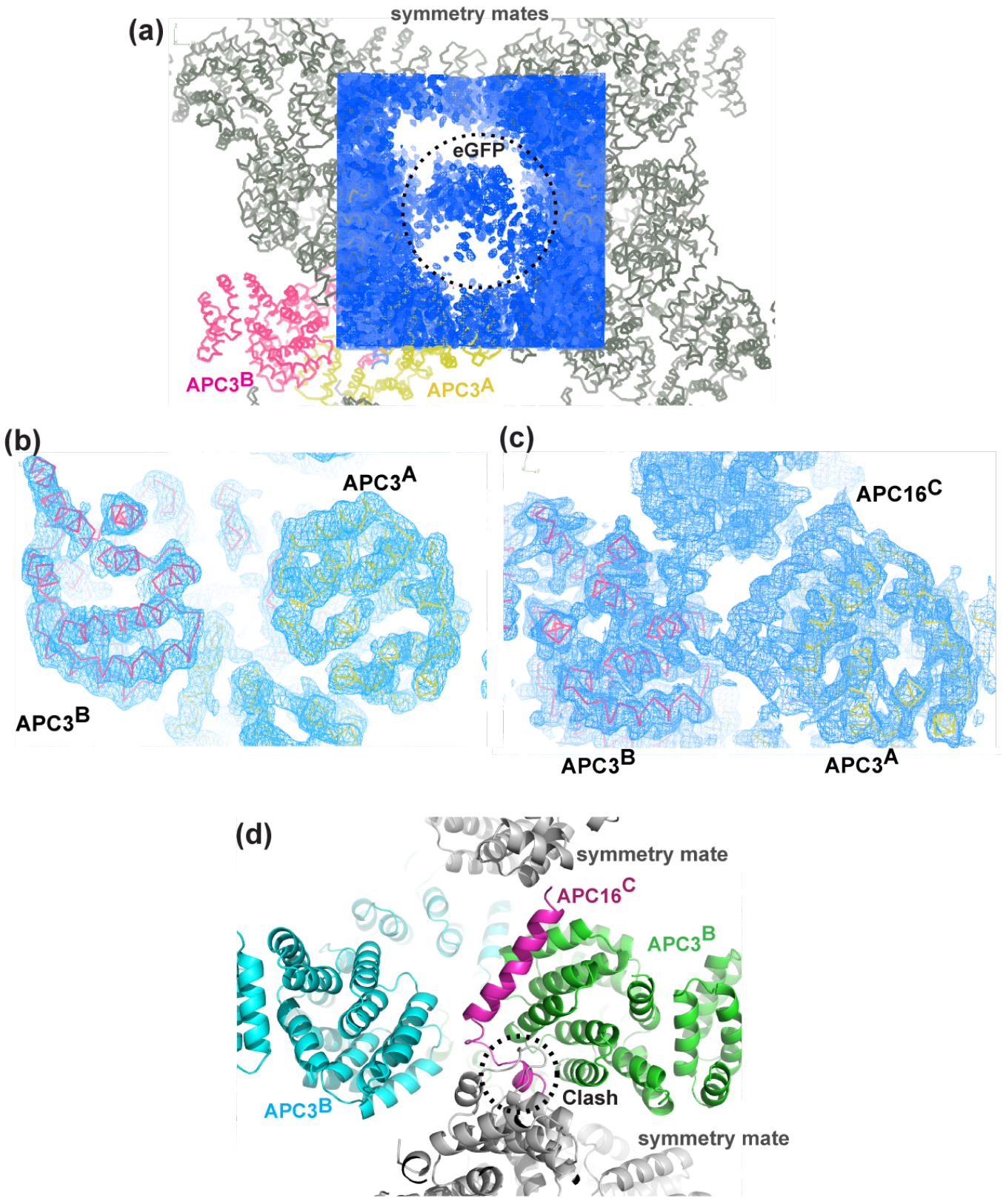
(a)
symmetry mates
eGFP
APC3B
APC3A
(b)
APC3A
APC3B
(c)
APC16C
APC3B
APC3A
(d)
symmetry mate
APC16C
APC3B
APC3B
Clash
symmetry mate

Figure S3. Electron density map and crystal packing of two crystal forms, $P4_3$ and $P6_5$

(a) Electron density map calculated from selenomethionine SAD phasing with density modification (for GFP-APC3ΔloopΔC20-APC16^C, see Materials and Methods). The dashed circle indicates weak electron density, which we attribute to the GFP fused at the N-terminus to APC3, but which we were unable to model. Note: anomalous difference maps generated at several stages of structure determination and model building did not yield obvious peaks for any of the six selenomethionines per GFP (12/au).

(b) Final 2Fo-Fc electron density from the $P6_5$ crystal form contoured at 1σ.

(c) Final 2Fo-Fc electron density from the $P4_3$ crystal form contoured at 1σ over the same region of APC3 as in b, highlighting the interface with APC3.

(d) Crystal structure of APC3Δloop (not shown)-APC16^C superimposed on structure of APC3Δloop including symmetry mates (grey). Crystal packing in the $P6_5$ crystal form precludes interaction with APC16^C due to occupation of the APC16^C binding site by symmetry mates.

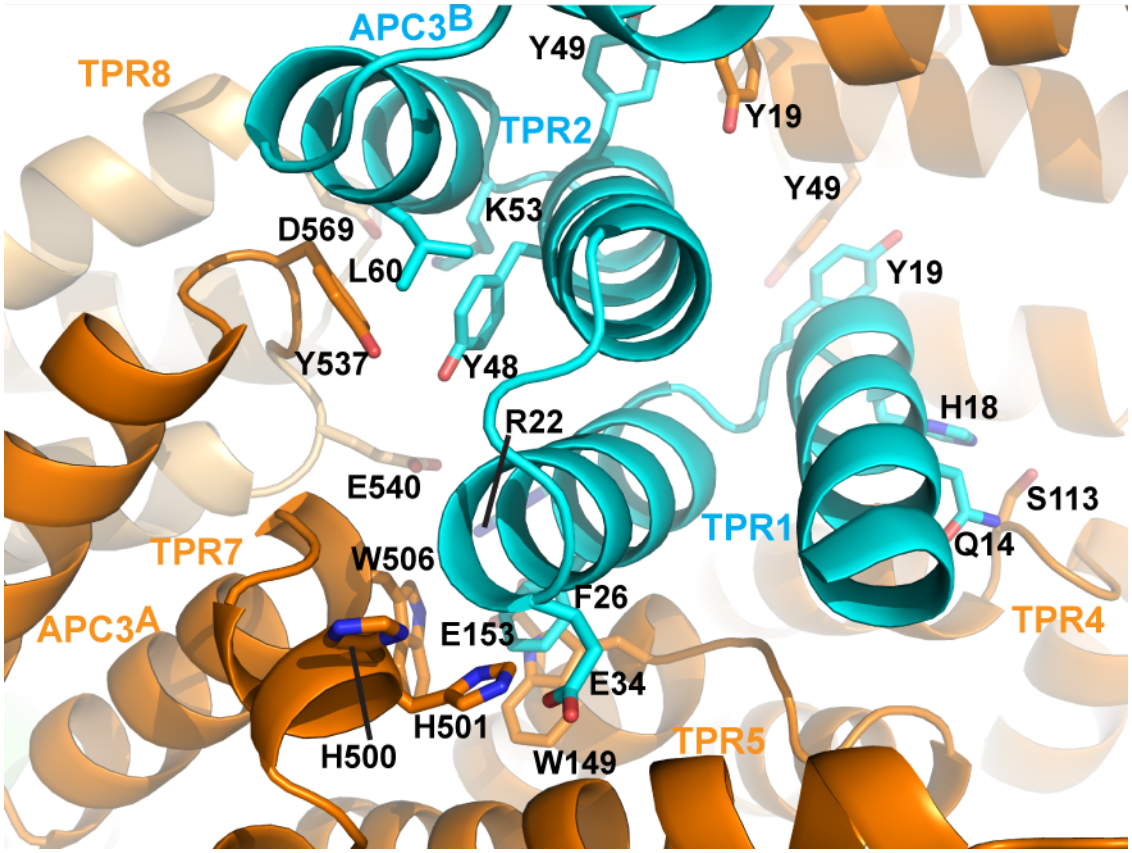

Figure S4. APC3 dimer interface
Close-up view of the APC3 dimer interface from the APC3Δloop-APC16^{C} structure. The color is same as in Fig. 2. Gln14, His18, Tyr19, Arg22, Phe26 and Glu34 from TPR1 in protomer "B" interact with Ser113 from TPR4 and Tyr49 from TPR2, Trp149 form TPR5, Glu540 from TPR7 and His500, His501 from TPR7 in in protomer "A". Tyr48, Lys53, Leu60 from TPR2 in protomer "B" interacts with Tyr537 from TPR7 and Asp569 from TPR8 in protomer "A".

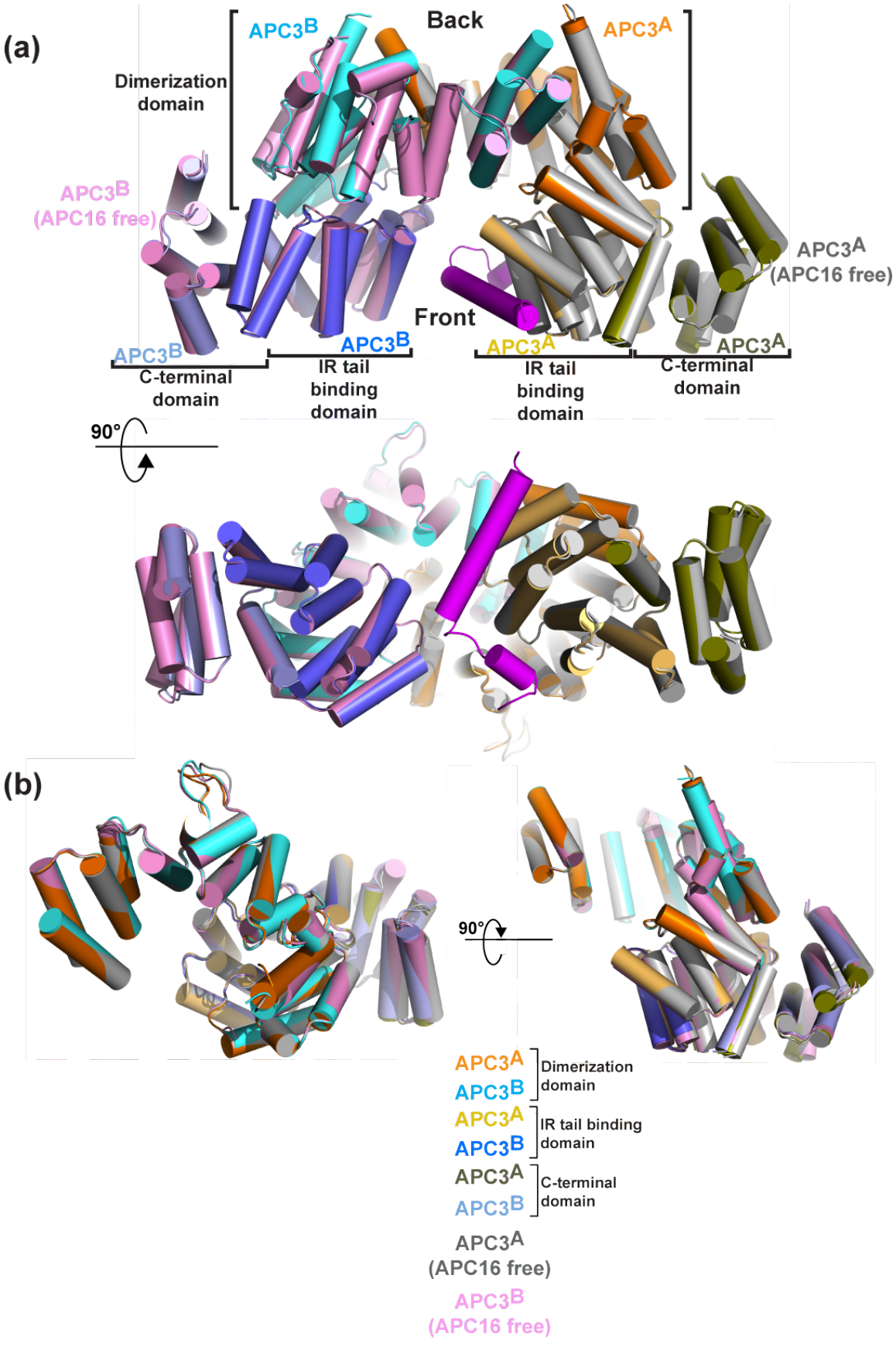
(a)
Back
APC3B
APC3A
Dimerization domain
APC3B (APC16 free)
APC3A (APC16 free)
Front
APC3B
APC3B
APC3A
APC3A
C-terminal domain
IR tail binding domain
IR tail binding domain
C-terminal domain
90°
(b)
90°
APC3A
APC3B
Dimerization domain
APC3A
APC3B
IR tail binding domain
APC3A
APC3B
C-terminal domain
APC3A (APC16 free)
APC3B (APC16 free)

Figure S5. Superimposition of the structures of APC3 alone and in complex with APC16

(a) Superimposition of the structures of APC3Δloop with and without $APC16^{C}$. The color for the structure of APC3 with APC16 is same as in Fig. 4. The structures of APC3 protomers A and B in the APC16-free form are colored gray and pink, respectively. The RMSD for APC3Δloop in the two crystal forms/with or without $APC16^{C}$ is 0.27 Å for 706 Cα.

(b) Superimposition of individual chains of the structures of APC3 with and without APC16. There is no apparent significant conformational change upon APC16 binding.

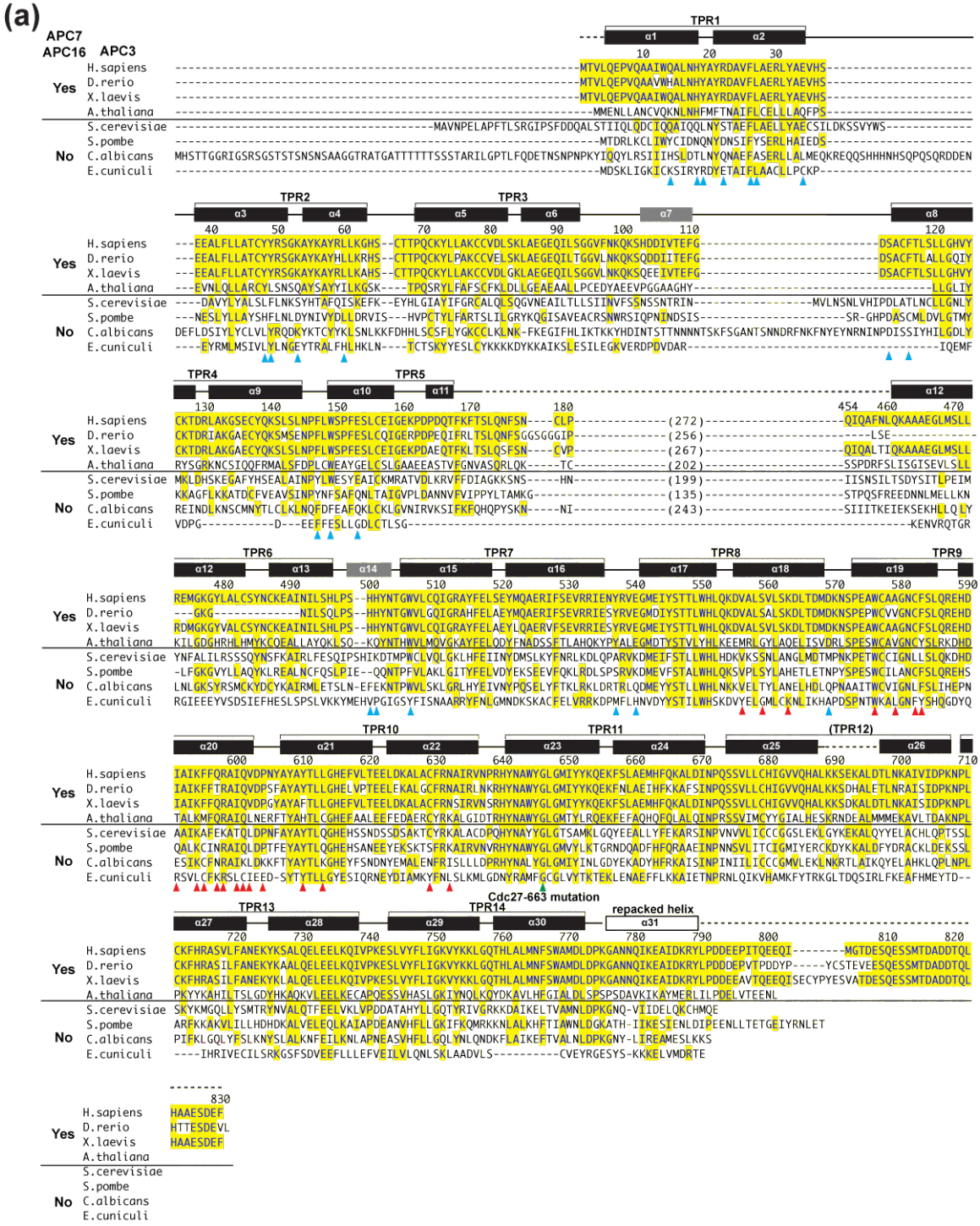
(a)
APC7
APC16
APC3
Yes
No
H.sapiens
D.rerio
X.laevis
A.thaliana
S.cerevisiae
S.pombe
C.albicans
E.cuniculi
TPR1
TPR2
TPR3
TPR4
TPR5
TPR6
TPR7
TPR8
TPR9
TPR10
TPR11
(TPR12)
TPR13
TPR14
repacked helix
Cdc27-663 mutation

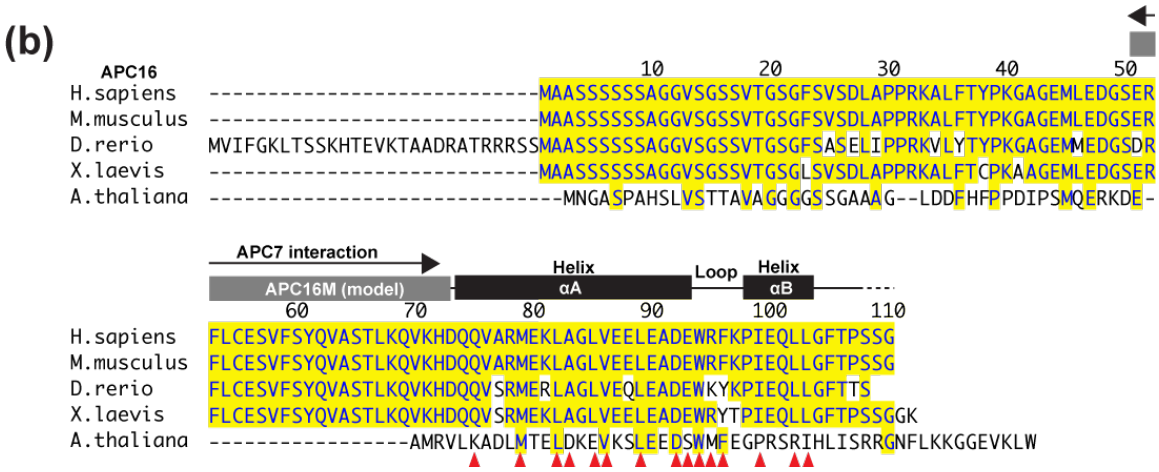

Figure S6. Sequence alignment of APC3 and secondary structure elements from crystal structure.

(a) Alignment of APC3 sequences from *H. sapiens*, *D. rerio*, *X. laevis*, *A. thaliana*, which have APC16 and APC7, and *S. cerevisiae*, *S. pombe*, *C. albicans*, and *E. cuniculi*, which do not have APC16 and APC7. Residues identical to human APC3 are colored yellow. Secondary structures are shown above the sequence with helix and TPR numbers based on the crystal structure of APC3Δloop. Residues involved in the dimer interface and APC16 interaction are indicated with blue and red triangles, respectively. The site corresponding to the *S. cerevisiae* Cdc27-663 mutation (Gly613 to Asp, equivalent to Gly646 in Human APC3) is indicated with a green triangle. Residues in APC3 loop are omitted for clarity.

(b) Alignment of APC16 sequences from *H. sapiens, M. musculus, D. rerio*, *X. laevis*, *A. thaliana* based on the structure of APC16^{C}. Secondary structures are shown above the sequence. The residues interacting with APC3 are indicated with red triangles.

Supplementary References

1. Buchan, D. W., Minneci, F., Nugent, T. C., Bryson, K. & Jones, D. T. (2013). Scalable web services for the PSIPRED Protein Analysis Workbench. *Nucleic Acids Res* **41**, W349-57.
2. Karpenahalli, M. R., Lupas, A. N. & Soding, J. (2007). TPRpred: a tool for prediction of TPR-, PPR- and SEL1-like repeats from protein sequences. *BMC Bioinformatics* **8**, 2.